EUROPHYSICS LETTERS Online First

Europhys. Lett. (2005)
DOI: 10.1209/epl/i2004-10504-y

Holographic scattering in the ultraviolet spectral range in iron-doped lithium niobate

M. A. Ellabban[1], Th. Woike[2], M. Fally[1](*) and R. A. Rupp[1]

[1] *Institut für Experimentalphysik, Universität Wien*
Boltzmanngasse 5, A-1090 Wien, Austria
[2] *Institut für Mineralogie, Universität zu Köln*
Zülpicherstr. 49b, D-50674 Köln, Germany

received 16 November 2004; accepted in final form 22 March 2005
published online 13 April 2005

PACS. 42.25.Fx – Diffraction and scattering.
PACS. 42.40.Ht – Hologram recording and readout methods.
PACS. 42.65.Hw – Phase conjugation; photorefractive and Kerr effects.

Abstract. – Photo-induced light scattering in iron-doped lithium niobate crystals is investigated at different wavelengths in the near ultraviolet spectral range. We observed a remarkable difference of the angular distribution of scattered light when changing the pump wavelength. These findings can be explained by the spectral dependence of the competing recording mechanisms photovoltaic effect and diffusion. We found that the magnitude of the photovoltaic effect is decreasing from 364 nm to 334 nm, and diffusion becomes the dominant charge transport mechanism for photorefraction.

Introduction. – Investigations of the photorefractive effect in lithium niobate in the near UV region of the spectrum are attractive for holographic recording and data storage as the photoconductivity increases and the photovoltaic field decreases in this spectral range [1–3]. This leads to faster photorefractive buildup times and easier control of hologram recording with the application of an external field as compared to the visible spectral range. Moreover, a higher gain is obtained at near UV wavelengths [4]. In general, photorefractive materials in the near UV open up an outstanding potential for applications that require high resolution such as image processing.

In the past, holographic recording in the near UV was investigated in lithium niobate [1,2], lithium tantalate [2,5,6], lithium iodate [7], KH_2PO_4 [8], Fe^{3+}-doped triglycine sulphate [9], and $Bi_4Ge_3O_{12}$ [10]. Only recently became the UV spectral range very attractive for holographic recording in nominally undoped, Mg-doped and doubly doped lithium niobate [11–15] for non-volatile memories. Light-induced domain engineering in lithium niobate comprises a further important feature of UV illumination. This is a method to strongly reduce the coercive field to half of its value [16–18]. However, excitation and trapping processes are unknown. Studies of holographic scattering (HS) in the UV spectral range were not conducted in any material up to now, though. In contrast, UV light was even used to suppress the effect of

(*) E-mail: martin.fally@univie.ac.at

parasitic holograms (PH) by a simultaneous illumination of the photorefractive crystal by UV light and the recording beam in the visible [19].

Beam propagation of laser light through any photorefractive material is usually accompanied by an unintentional gradual increase of light-induced scattering, so-called HS. The generation of such PH takes place together with the desired hologram and even occurs if only a single beam is incident on the crystal. This is due to interference between the pump beam and its own scattered waves from irregularities at the crystal surfaces or inhomogeneities within the crystal. Subsequently, small refractive-index changes, *i.e.* PH, are induced via the photorefractive effect. Finally, the weak initially scattered beams are amplified at the expense of the pump beam provided that the former interferes constructively with the self-diffracted wave. As the presence of PH strongly deteriorates the quality of the desired hologram, we investigate HS in the near UV in a model photorefractive crystal —lithium niobate— that is well studied in the visible range, in order to complete the insight view, especially into the charge transport processes [20, 21].

It is well established that in the visible spectral range the photorefractive effect in iron-doped lithium niobate is mainly governed by the *bulk photovoltaic effect* together with a marginal contribution of *diffusion*. The absorption band around 2.6 eV was assigned to intervalence transitions Fe^{2+}-Nb^{5+}, that are responsible for the photorefractive effect in iron-doped lithium niobate [22], and the photovoltaic current density is linearly proportional to the concentration of those Fe^{2+} centers [23]. Here, we apply HS as a technique to study photorefractive properties. HS experiments have some major advantages over other holographic techniques: they are simple to perform and insensitive to mechanical vibrations of the optical system [24]. In addition, the complete reciprocal-space is mapped, *i.e.*, projected, onto a screen *at once*.

The aim of this letter is to demonstrate the appearance of HS in the near UV and to characterize it at the example of iron-doped lithium niobate. The holographic scattering pattern for three distinct wavelengths, $\lambda_p = 334$, 351, 364 nm, at the high-energy side of the 2.6 eV absorption band is monitored. We find that the three scattering distributions differ dramatically. Analyzing the distributions we are able to attribute this feature to changes of the relative contributions of the photovoltaic effect (PVE) and the diffusion process to the photorefractive effect. Finally, the angular dependence of the transmitted intensity in the presence of PH is investigated for those wavelengths.

Experiment. – The investigations were performed on a single crystal of $LiNbO_3 : Fe$ with $7.46 \times 10^{23}\,m^{-3}$ concentration of Fe^{2+}. The crystal is a plane-parallel plate with dimensions $5.5 \times 1.3 \times 6.5$, the thickness being $d = 1.3$ mm. The polar c-axis is lying in a plane perpendicular to the surface normal. The sample was partially reduced with a ratio $Fe^{2+}/Fe^{3+} > 0.08$, so that photo-conduction is due to electrons only [2]. The light of an extraordinarily polarized Ar^+ ion laser beam was employed to record PH at $\lambda_p = 364$ nm, 351 nm or 334 nm, respectively, with a recording intensity of $I = 35\,mW/cm^2$. Thereby the recording beam impinges perpendicularly onto the crystal surface. By a combination of $\lambda/2$ plate and a polarizer, the polarization and the intensity of the pump beam were adjusted. The scattering pattern, projected onto a standard fluorescent screen for UV light placed behind the crystal, was registered by a CCD camera. During the reconstruction of PH at different angles the power of the laser beam was reduced in order not to affect the recorded holograms and keeping the polarization state unchanged as compared to recording. The sample is placed on an accurately controlled rotation stage ($\pm\,0.001°$) when performing rocking curves, *i.e.* transmitted intensity as a function of the rotation angle of the crystal. Absorption spectra of the sample were collected using a Cary 500 photo-spectrometer.

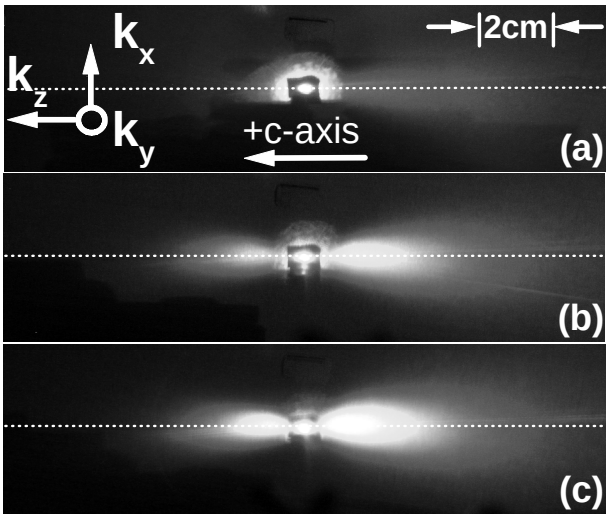

Fig. 1 – Far-field intensity distribution of the amplified scattered light for pump beams of different wavelengths (a) $\lambda_p = 334$, (b) 351 and (c) 364 nm. The $+c$-axis of the crystal points to the left. The pump beam is centered at the crystal visible as a dark rectangular contour. The fluorescent screen was placed at a distance of 4.5 cm behind the sample. The scale is valid for the height and the width of the screen for all photos.

Results and discussion. – Figure 1 displays the steady-state far-field scattering patterns recorded for three wavelengths in the UV in a plane perpendicular to the [010]-direction. We relate the laboratory system and the crystallographic coordinate system by [010] $\parallel k_y \parallel a$-axis and [001] $\parallel k_z \parallel c$-axis. The scattered intensity distributes asymmetrically along both directions of the c-axis, but preferentially along the $-c$-axis similarly as in the visible spectral range [25]. Note that the width of the transmitted beam increases with decreasing wavelength (bright spot at the center). This might be due to a thermal lens effect of the sample that depends on the wavelength through the absorption. The obvious asymmetry of the scattering pattern along both directions of the c-axis results from the competition of the diffusion and PVE contribution to the charge transport processes. On the one hand, diffusion leads to a unidirectional amplification and thus to high scattering intensity only along *one direction* of the c-axis. This direction depends on the sign of the electro-optic coefficient and the type of charge carriers [26]. Here, electrons are the charge carriers and the electro-optic coefficient is positive, so that light is amplified along the $-c$-axis. On the other hand, the PVE contribution cannot lead to a steady-state energy transfer between the pump and scattered beams, but only to a transient energy transfer. This is due to the interaction between beams of dissimilar intensities, for which energy transfer always occurs from the strong to the weak beam [27]. As the weak scattered beams are assumed to be symmetrically distributed around the pump beam, a symmetric amplification of the scattered beams in *both directions* of the c-axis occurs, along which a high electro-optic coefficient, r_{33}, acts. Due to these diverse types of amplification an asymmetry in the scattering pattern shows up, depending on the relative contributions of PVE and diffusion. It can be seen in fig. 1 that the asymmetry of the scattering pattern increases with decreasing λ_p.

To explain this behavior, let us consider the absorption spectrum of the investigated sample shown in fig. 2. The vertical solid lines at 364, 351 and 334 nm indicate the Ar^+ laser lines

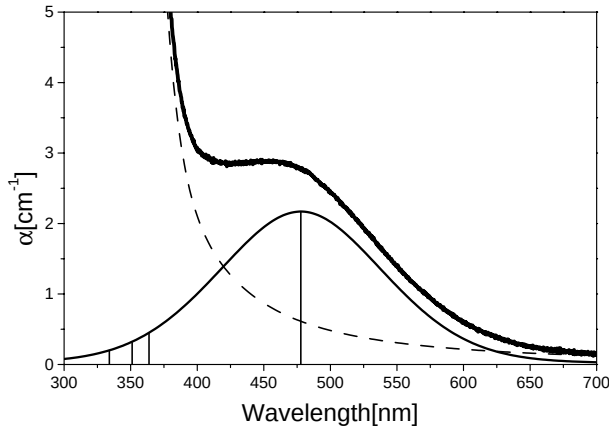

Fig. 2 – Absorption spectra of the investigated crystal for extraordinarily polarized light. The lines represent a Gaussian/Lorentzian fit for the absorption bands due to Fe^{2+} (solid line) and the charge transfer from oxygen π-orbitals to Fe^{3+} (dashed line).

and the center of the Fe^{2+} absorption band at 477.8 nm, respectively. The latter was fitted by a combination of Gaussian and Lorentzian functions, accounting also for another strong band around 4 eV, that is assigned to charge transfer from oxygen π-orbitals to Fe^{3+} ions [23]. The absorption coefficient α for the Fe^{2+} band decreases from 364 to 334 nm. The decisive quantity of the photorefractive effect is the photovoltaic field $E_{PV} = -\alpha G I/\sigma$, where I, G and σ are the light intensity, the Glass constant and the photoconductivity, respectively. Thus E_{PV} depends on the spectral dependence of G, α and (I/σ). The Glass constant is known to exhibit a broad maximum in the Fe^{2+} excitation region of partially reduced crystals centering at 3 eV [28]. To access the spectral dependence of (I/σ), we studied the exposure dependence of HS by monitoring the decrease of the transmitted intensity as shown in fig. 3. The solid lines are fitting curves using an equation from ref. [29], that models the amplification

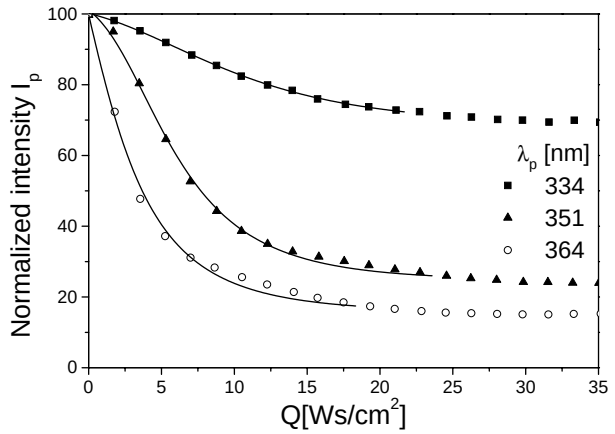

Fig. 3 – Exposure dependence of the transmission during recording of PH using an extraordinarily polarized laser beam at λ_p of 334, 351 and 364 nm. The solid lines are fitting curves employing eq. (6) from ref. [29].

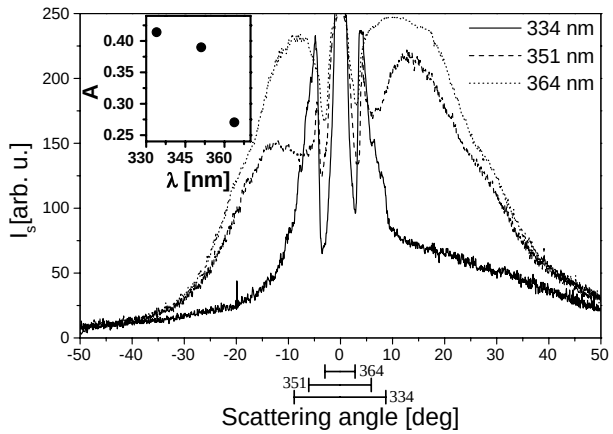

Fig. 4 – Scattered intensity distribution along k_z at $k_x = 0$ (white dotted lines in fig. 1). The inset presents the asymmetry parameter A for the scattering patterns at three UV wavelengths. The central peak corresponds to the transmitted beam, side minima for 351 and 334 nm nearby are due to the crystal edges. For the calculation of A the regions, that are influenced by the transmitted beam and are indicated by bars below, were discarded.

of PH. The relaxation time constant τ then yields the photoconductivity $\sigma = \epsilon\epsilon_0/\tau$, with ϵ and ϵ_0 the permittivities of the medium and vacuum, respectively. We find that at constant pump intensity (I/σ) decreases with increasing wavelength in the UV range. However, the relative changes of (I/σ) at different wavelengths are much less than that of α and G, so that the overall value of the photovoltaic field decreases towards lower wavelengths in the near UV as directly detected by ESR [3]. From our measurements (figs. 2 and 3) and using the Glass constants from ref. [30], we get $E_{PV} = 394$, 840, 1620 V/cm for $\lambda = 334$, 351, 364 nm, respectively. Hence the asymmetry of the scattering pattern must increase with decreasing wavelength in accordance with our observation (see fig. 1).

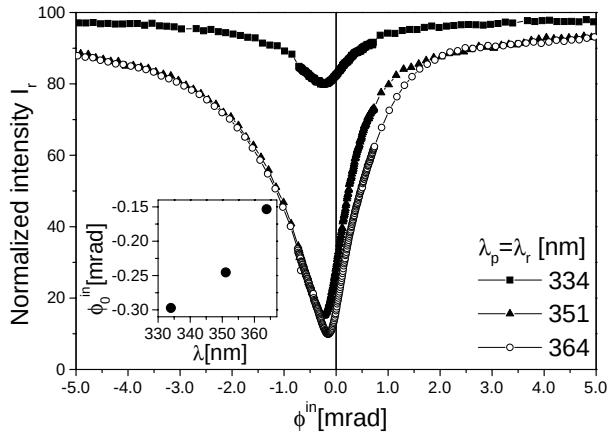

Fig. 5 – The angular dependence (ϕ-rotation) of the normalized transmitted intensity I_r during reconstruction of PH recorded in the crystal at $\lambda_p = 334$, 351 and 364 nm. The superscript "in" indicates that the rotation angle is given within the crystal.

In order to find a quantitative measure for the asymmetry of the scattered intensity along the c-axis, we analyzed the two-dimensional scattering patterns displayed in fig. 1 along k_z at $k_x = 0$, indicated by the dotted line. The resulting curves, shown in fig. 4, were employed to calculate the asymmetry parameter A. The latter is defined as the ratio between the difference and the sum of the integrated scattered intensities along the $+c$ and $-c$-direction, respectively [31]. Thus, for perfect symmetry $A = 0$ and complete asymmetry $A = 1$. The inset of fig. 4 shows A as a function of λ_p which decreases with increasing wavelength as expected. Again, this is due to the spectral dependence of the relative contribution of the PVE and diffusion.

To give another independent measure for the ratio of contributions, we monitored the angular selectivity of the recorded PH. This was done by measuring the transmitted intensity of the read-out beam, normalized to the transmitted intensity at large angles, where it saturates as a function of the rotation angle ϕ as shown in fig. 5. As one remarkable feature, the position ϕ_0 of lowest transmitted intensity does not occur at the recording angle, but is slightly shifted towards the negative sense of rotation. This was shown to be characteristic for diffusion [32]. The deviation from the recording angle increases with decreasing wavelength (inset), a fact that supports the interpretation of the results shown above. The essential features can be understood in the frame of an Ewald-sphere construction model described in detail in refs. [20, 32].

Summary. – In summary, we conducted the first study of HS in an iron-doped lithium niobate crystal in the near UV spectral range. We found that the structure of the scattering pattern strongly depends on the pump wavelength. This can be explained by the spectral dependence of the photovoltaic field, extracted from our measurement. Here, we applied HS as a simple technique to probe the contributions of the PVE and diffusion to the photorefractive effect in the near UV. The PVE decreases with decreasing recording wavelength and diffusion becomes the dominant recording mechanism. Higher gains, *e.g.*, $33.6\,\mathrm{cm}^{-1}$ at 351 nm, and shorter time constants are obtained in the near UV in comparison to the visible spectral range.

* * *

Financial support by the Austrian science foundation FWF (P-15642) is gratefully acknowledged. We thank Prof. E. Tillmanns for continuous support.

REFERENCES

[1] Krätzig E., *Ferroelectrics*, **21** (1978) 635.
[2] Orlowski R. and Krätzig E., *Solid State Commun.*, **27** (1978) 1351.
[3] Schirmer O. F., Juppe S. and Koppitz J., *Cryst. Latt. Def. Amorp.*, **16** (1987) 353.
[4] Jungen R., Angelow G., Laeri F. and Grabmaier C., *Appl. Phys. A*, **55** (1992) 101.
[5] Dittrich P., Koziarska-Glinka B., Montemezzani G., Günter P., Takekawa S., Kitamura K. and Furukawa Y., *J. Opt. Soc. Am. B*, **21** (2004) 632.
[6] Bernasconi P., Montemezzani G., Günter P., Furukawa Y. and Kitamura K., *Ferroelectrics*, **223** (1999) 373.
[7] Sun Q., Rupp R. A., Fally M., Vietze U. and Laeri F., *Opt. Commun.*, **189** (2001) 151.
[8] Laeri F., Jungen R., Angelow G., Vietze U., Engel T., Würtz M. and Hilgenberg D., *Appl. Phys. B*, **61** (1995) 351.
[9] Montemezzani G., Fousek J., Günter P. and Stankowska J., *Appl. Phys. Lett.*, **56** (1990) 2367.
[10] Montemezzani G., Pfändler St. and Günter P., *J. Opt. Soc. Am. B*, **9** (1992) 1110.

[11] Tomita Y., Sunarno S. and Zhang G., *J. Opt. Soc. Am. B*, **21** (2004) 753.
[12] Ling F., Wang B., Guan Ch X., Tao G., Dong T. D., Yuan W. and Sun N., *Opt. Commun.*, **241** (2004) 293.
[13] Zuo W., Matsushima R., Tomita Y. and Zhang G., *Jpn. J. Appl. Phys.*, **43** (2004) 7491.
[14] Lee M., Kim I. G., Takekawa S., Furukawa Y., Uchida Y., Kitamura K. and Hatano H., *J. Appl. Phys.*, **89** (2001) 5311.
[15] Lee M., Takekawa S., Furukawa Y., Kitamura K., Hatano H. and Tao S., *Opt. Lett.*, **25** (2000) 1337.
[16] Wengler M. C., Fassbender B., Soergel E. and Buse K., *J. Appl. Phys.*, **96** (2004) 2816.
[17] Fujimura A., Sohmura T. and Suhara T., *Electron. Lett.*, **39** (2003) 719.
[18] Müller M., Soergel E. and Buse K., *Appl. Phys. Lett.*, **83** (2003) 1824.
[19] Youwen L., Jayavel R., Nakamura M., Kitamura K., Yamaji T. and Hatano H., *J. Appl. Phys.*, **92** (2002) 5578.
[20] Fally M., Ellabban M. A., Rupp R. A., Fink M., Wolfsberger J. and Tillmanns E., *Phys. Rev. B*, **61** (2000) 15778.
[21] Ellabban M. A., Rupp R. A. and Fally M., *Appl. Phys. B*, **72** (2001) 635.
[22] Dischler B., Herrington J. R., Räuber A. and Krätzig E., *Solid State Commun.*, **14** (1974) 1233.
[23] Krätzig E. and Schirmer O., *Photorefractive Materials and their Applications I*, edited by Günter P. and Huignard J.-P., Vol. **61** (Springer-Verlag, Berlin) 1988, p. 131.
[24] Ellabban M. A., Mandula G., Fally M., Rupp R. A. and Kovács L., *Appl. Phys. Lett.*, **78** (2001) 844.
[25] Goulkov M., Odoulov S., Woike Th., Imbrock J., Imlau M., Krätzig E., Bäumer C. and Hesse H., *Phys. Rev. B*, **65** (2002) 195111.
[26] Petrov M. P., Stepanov S. I. and Khomenko A. V., *Photorefractive Crystals in Coherent Optical Systems*, Vol. **69** (Springer-Verlag, Berlin) 1991, p. 50.
[27] Vinetskiĭ V. L., Kukhtarev N. V., Odulov S. G. and Soskin M. S., *Sov. Phys. Usp.*, **22** (1979) 742.
[28] Krätzig E. and Kurz H., *J. Electrochem. Soc.*, **124** (1977) 131.
[29] Rupp R. A. and Drees F. W., *Appl. Phys. B*, **39** (1986) 223.
[30] Sturman B. I. and Fridkin V. M., *The Photovoltaic and Photorefractive Effects in Noncentrosymmetric Materials*, Vol. **8** (Gordon and Breach Science Publishers, Philadelphia) 1992, p. 135.
[31] Imlau M., Goulkov M., Fally M. and Woike Th., *Polar Oxides: Properties, Characterization and Imaging*, edited by Böttger U., Tiedke St. and Waser R. (Wiley, Berlin) 2004, p. 163.
[32] Ellabban M. A., Fally M., Imlau M., Woike Th., Rupp R. A. and Granzow T., *J. Appl. Phys.*, **96** (2004) 6987.